Promoting Materials Science and Engineering Education through 3D Printing Technology

Dr. Tracy Zhang, MSU

Michigan State University (MSU) St. Andrews, Midland, MI. Dr. Tracy Zhang is a faculty member and STEM Outreach Specialist at Michigan State University St. Andrews campus. She earned a doctoral degree in advanced materials from Central Michigan University. Her current role involves promoting STEM education to K-12 students focusing on 3D printing technology area and conducting research in the development of biosourced hyperbranched poly(ester)s for the controlled release of actives across a range of applications.

Dr. Robert Allen Bubeck, Michigan State University - St. Andrews

Dr. Robert A. Bubeck is currently a Research Assistant Professor at Michigan State University in Midland, Michigan with over 44 years of experience in industrial research and development. He is a graduate of Drexel and Cornell Universities. Research areas include the development of new liquid crystalline polymers, semi-crystalline polymers, thermoplastics, hyperbranched polymers, and dendrimers. He has broad-based expertise in the areas of structure/property fundamentals, mechanical behavior, composites and blends, rheology, fiber spinning, 3D additive fabrication, surface science, and interfaces. Prior to joining the Michigan State University, Dr. Bubeck pursued research in materials and polymer science at the Dow Chemical Company where he attended the level of Fellow, and at Michigan Molecular Institute. Within the Dow research community, he pioneered synchrotron-based research aimed at the advanced characterization of the physical behavior, surfaces, and processing of polymers. He is an author or co-author of over 62 publications and 5 patents. He has presented invited talks at major institutions such as Cornell University, MIT, University of Massachusetts, Case Western Reserve University, the University of California at Santa Barbara, and the University of Minnesota. Dr. Bubeck is a Senior Fellow of the American Physical Society.

Miss Therese Aimei Joffre, Midland High School
Ms. Grace Anne Bremmer , H. H. Dow High School

H. H. Dow High School, Midland, MI. Grace was a rising senior when taking the research internship at MSU St. Andrews.

Mr. Logan Patrick McNamara, H. H. Dow High School, Midland, MI

Logan was a rising senior when taking the research internship at MSU St. Andrews.

Aaron Michael Heydenburg
Prof. Bingbing Li, Department of Chemistry and Biochemistry, Central Michigan University

Prof. Bingbing Li (the corresponding and presenting author), the Department of Chemistry and Biochemistry, Central Michigan University. Dr. Li is an Associate Professor of Chemistry at Central Michigan University. She received her doctoral degree in Chemistry from Virginia Tech. Dr. Li's research primarily focuses on the design of hierarchically structured polymeric materials for biomedical and environmental applications, with an emphasis on the design and property optimization of these polymer-based materials. Dr. Li has also been actively involved in macromolecular science and engineering education. She served as a research advisor for the summer interns at MSU St. Andrews during summer 2019.

Promoting Materials Science and Engineering Education through 3D Printing Technology

Abstract

In 2015, the Michigan State Board of Education voted to adopt new Michigan Science Standards that heavily draw on the Next Generation Science Standards (NGSS). Among all the performance expectations from these science standards, incorporating high school engineering design requires more effective collaboration between K-12 teachers, higher educators, scientists, and engineers. Without such collaborative effort, K-12 teachers could face tremendous challenges for the design and implementation of meaningful engineering education lessons that could meet the standards. Summarized in this paper are the design and implementation of materials science and engineering educational research offered to high school rising seniors in summer 2019. The summer training program provides students an opportunity to learn the design criteria for fabricating bone scaffolds and to gain capability of breaking down a complex real-world problem into small problems that can be answered in laboratory set-up, which meet both the Michigan State Science Standards and the Next Generation Science Standards. Through this summer training program, students learned to relate the structures of several polymers to their physical properties, design 3D objects with various geometrical infills by using computer aided design (CAD) and slicing software, fabricate 3D-pringting objects, perform compression tests, analyze stress-strain characterization results, conduct statistical life data analysis, and relate research results to real-world problems.

Introduction

Injuries and diseases of musculoskeletal tissues are common across all age groups. Some of these conditions require the removal of shattered or malignant bone tissues and result in bone defects. Small bone defects can heal spontaneously through a regenerative healing process which follows cellular and molecular mechanisms similar to those for the formation of embryonic bone.[1,2] However, bone defects larger than a critical size cannot heal spontaneously via the regenerative healing process. Critical-sized bone defects are generally defined as those greater than 1-2 cm or those correspond to greater than 50% loss of the bone circumference, depending on the anatomic location of the host tissue.[3–5] Critical-sized bone defects, both congenital and acquired, are

serious and costly impairments. To induce the bone regeneration across critical-sized defects, surgical intervention and therapeutic agents are usually required. A common approach proposed in regenerative medicine is to implant a biomaterial scaffold at the injured site to promote bone regeneration by attracting cells to the area.[6] Synthetic and natural biomaterial scaffolds with structures that mimic the architecture of the host bone site can provide an essential framework for cell adhesion, migration, and proliferation, as well as the possible induction of bone morphogenic process.[1,2,6] Additive manufacturing techniques have been widely used as scaffold fabrication methods due to their affordability and potential to create complex geometries and internal structures using various polymeric filaments.[7–9] In particular, 3D printing allows customized design and fabrication of scaffolds that can meet specific needs of each patient. Therefore, 3D printing has been heavily studied for prototyping tissue scaffolds that can mimic the mechanical strength and biological environment of host bone tissues.[8–10]

An eight-week summer project on 3D printed bone materials was designed for aspiring high school rising seniors who are interested in biomaterials and engineering research. In this project, the Fused Deposition Modelling (FDM) 3D printing technique was used for the fabrication of bone scaffold models using various polymer and biopolymer filaments. Polymer scaffolds ($1\times1\times1$ cm^3 cubes) with different infill geometries and densities were fabricated. The mechanical properties of these scaffolds were characterized using compression tests to determine the yield stresses and compressive Young's moduli. The reliability of the mechanical behavior of the scaffolds was evaluated by determining the probability of failure via Weibull statistical analysis. The mechanical test results were further compared with the yield stresses and moduli of different trabecular bone tissues at multiple anatomical locations. All the above-mentioned research activities took place in an active-learning environment in well-equipped and professionally regulated scientific research laboratories. The summer program exposed the interns to a cutting-edge research topic on bone biomaterials and engaged them in formulating relevant research questions through literature study and seeking solutions through laboratory experiments. All interns were supervised by experienced faculty advisors, who provided research guidance and help them relate the summer experience to their research interests, college applications, and career paths. Overall, the results of this project not only provided for insight into the selection of polymer materials and the design criteria of scaffolds (e.g., the geometry and density of infill)

but also exposed high school rising seniors to a highly interdisciplinary research area in the science, technology, engineering, art, and mathematics (STEAM) fields. Both the education and research outcomes of this summer training program are presented, herein.

Program Description

Training Module 1. Characterization of Polymer Filaments

The Next Generation Science Standards encourages high school students to develop research skills such as analyzing data from material testing and describing material properties based on experimental results. However, high school students rarely have opportunities to access modern scientific instruments in order to enhance these research skills. In this training module, four high school rising seniors received training on two common polymer characterization techniquess: size exclusion chromatography (SEC, Malvern Panalytical, Westborough, MA, USA) and differential scanning calorimetry (DSC, TA Instruments, New Castle, DE). Students were trained to operate a Q20 DSC instrument, collect raw data from both SEC and DSC, and tabulate their results for presentations.

Polylactic acid (PLA), polylactic acid/polyhydroxyalkanoates (PLA/PHA), and polyvinyl alcohol (PVA) filaments were purchased from the same vendor (MatterHackers Inc., Lake Forest, CA) and used as received. Polycaprolactone (PCL) (3D4makers, Haarlem, Netherlands) and olefin block copolymer (OBC) (a gift from Dow Chemical Company, Midland, MI) filaments were also used, as received. Size exclusion chromatography experiments were performed by a faculty advisor to determine the molecular weights of the different polymers. The experiments were performed using two Agilent PLgel 3 μm mixed-E columns. Filament sample was dissolved in tetrahydrofuran (THF), with a typical concentration of approximately 1.0 mg/mL. The sample solutions were filtered using a 0.2 μm pore size filter to remove any particles prior to characterization. The DSC was operated by students to determine glass transition temperatures and melting points. Samples, contained in standard aluminum pans, were analyzed using a heating rate of 10 ºC/min. The sample compartment was purged with dry nitrogen at 50 cm^3/min during analysis. Students were also trained to use TA Universal Analysis software for analyzing the raw thermograms.

Table 1. Molecular weights, glass transition temperatures, and melting points of polymer filaments used in this study.

Materials	Mw (kDa)	T_g (°C)	T_{m1}(°C)	T_{m2}(°C)
PLA	129.8	57	149	NA
PLA/PHA	138.5	54	148	170
PVA	NA	61	182	NA
PCL	55.3	-61	62	NA
OBC	NA	46	108	138

SEC and DSC results are listed in **Table 1**. PCL, PLA, and PVA filaments were determined to have melting temperatures (T_{m1}) of 62°C, 149°C, and 182°C, respectively. Both PCL and PLA are biodegradable and biocompatible polyesters. PVA is a water-soluble synthetic polymer. The formulation of PVA filament was not provided by the vendor. PLA/PHA filament exhibits two melting points of 148°C and 170°C for PCL and PHA, respectively. PHA is a biodegradable polyester produced in nature by bacterial fermentation.[11] The combination of PLA and PHA can increase the toughness while retaining layer adhesion during 3D printing.[12] OBC filament was formulated by the Dow Chemical Company and made from a unique lightweight polyethylene-based material. The OBC material exhibits superior dimensional stability and chemical resistance, as well as excellent printability.[13] Two melting points are observed for OBC filament reflecting an unknown composition. A glass transition temperature (Tg) was not observed in the DSC thermogram of OBS filament because the Tg of this polyolefin is below -90°C, which is the lower limit of the Q20 DSC instrument. Through this training module, students gained confidence to (1) learn basic concepts about polymers and polymer characterization methods, (2) operate research instruments, (3) carry out a literature study, (4) graph, tabulate, and analyze raw data, and (5) correlate research results to the properties and functions of polymeric materials.

Training Module 2. 3D Printing Cubic Scaffolds

Cubic scaffold samples were printed using Flashforge Dreamer 3D printers (Flashforge 3D Technology Co. Jinhua City, China). The Flashprint (slicing software) settings for different types of filaments are tabulated in **Table 2**. The scaffold models were designed as $1\times1\times1 cm^3$ cubes using Onshape cloud-based CAD software. Rectilinear, triangle, hexagon, and gyroid configurations were used to template the infills of these cubic scaffolds. The cubic models with

Table 2. Flashprint settings for different types of filaments

Filament	T_{Nozzle}(°C)	T_{Bed}(°C)	Speed (mm/s)	Retraction Length (mm)	Retraction Speed (mm/s)
PLA	200	50	60	1.3	30
PLA/PHA	200	50	60	1.3	30
PVA	200	50	30	2.3	70
PCL	80	30	20	2.3	70
OBC	180	80	10	1.3	30

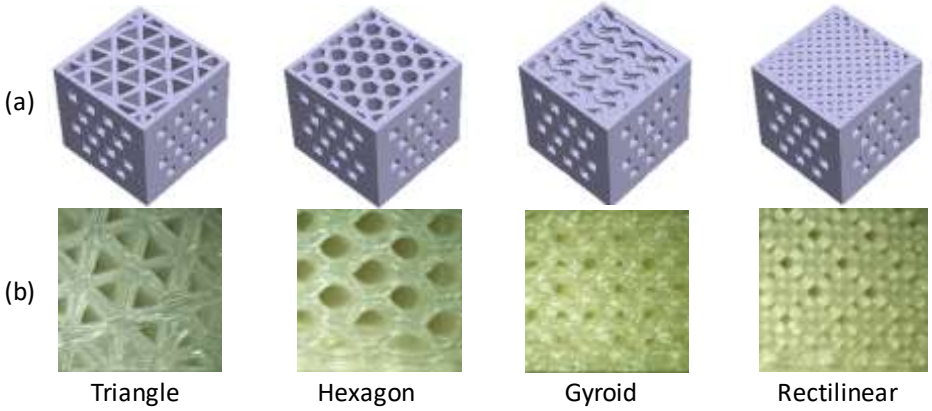

Figure 1. (a) Slicing models and (b) optical micrographs (OBC) for 3D-printed scaffolds with different geometrical infill patterns.

different infill geometries and densities were sliced using Flashprint slicing software to generate G-Code, a computer language that guides the motion controller during 3D printing. Slicing models with different infill geometrical patterns are shown in **Figure 1(a)**. During a 3D printing process, each Flashforge Dreamer 3D printer is able to simultaneously print six cubic scaffolds for materials other than PCL. Inconsistency in the appearance of samples was observedwhen multiple PCL samples were printed simultaneously using one 3D printer.PCL scaffolds were subsequently printed singly. Optical micrographs in **Figure 1(b)** show top views of OBC scaffolds with different geometrical infill patterns.

In this training module, a brief lecture about the 3D printing technique was presented by a faculty advisor. This was followed by student hands-on practice using CAD design and 3D printing. Four students worked as two groups with assigned filaments. Cubic scaffolds from different filaments (~1.75 mm diameter) were successfully printed after trial and error. The Flashprint configuration was optimized by students for 3D printing using each type of polymer

filament, as summarized in **Table 2.** Through this process, students also learned the implications of trial and error during scientific exploration.

Training Module 3. Compression Testing

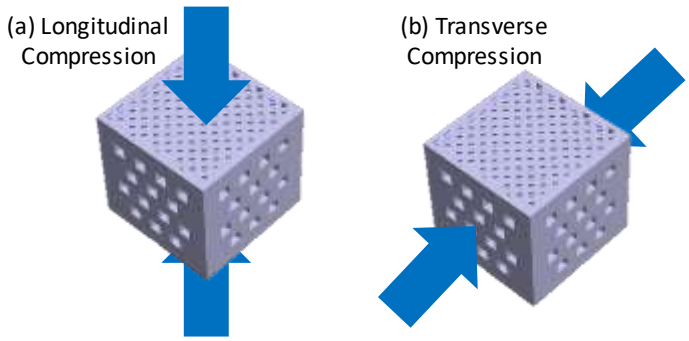

Figure 2. Illustrations of mechanical tests performed via (a) longitudinal or (b) transverse compression.

For scaffold samples prepared in Training Module 2, compression testing was carried out using a MTS Insight 5 Mechanical testing system (MTS, Eden Prairie, MN) with a compression rate of 1 mm·min^{-1} according to the ASTM D 1621 test standard.[14] The dimensions of each specimen were first measured and recorded. The specimen was then placed between two fixtures of the MTS Insight 5 mechanical tester fitted with MTS Bionix compression platens (50 mm diameter) and a 10 kN load cell. The cubes were compressed to the desired extension (2 mm). For each type of polymeric material, both longitudinal and transverse compression tests were performed as illustrated in **Figure 2**. Each experiment was repeated six times using six scaffolds. [Note: In order to gain confidence with Weibull statistical analysis, 30 replicates were obtained. The Weibull analysis is discussed later in the description of Training Module 4.] Stress-strain curves thus obtained from each compression test were used to determine the yield stress, defined as the point at which 2% plastic deformation occurs, and the compressive Young's modulus (*i.e.*, the slope of the Hookean region of a stress-strain curve) of each scaffold sample. Examples of stress-strain curves for OBC and PVA scaffolds are provided in **Supporting Materials**.

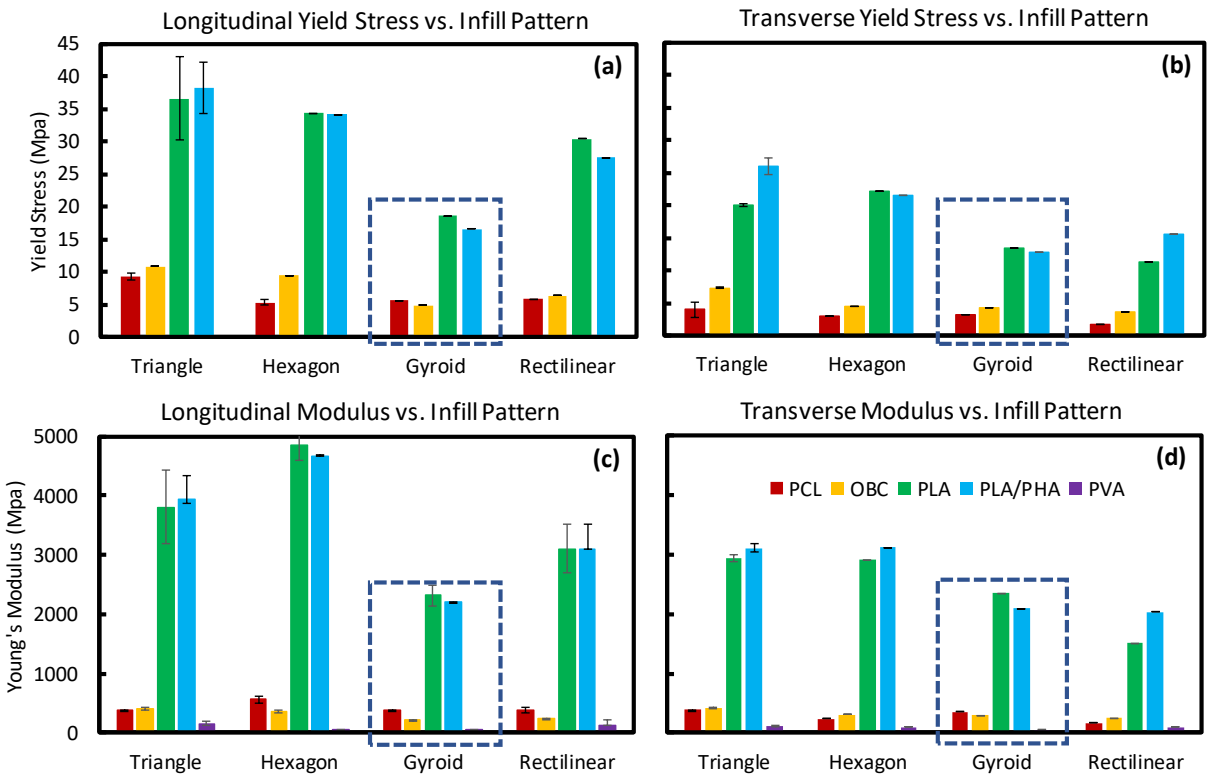

Figure 3. (a and b) Yield stresses (± standard deviation) and (c and d) compressive Young's moduli (± standard deviation) determined from longitudinal and transverse compression tests. All scaffolds were printed with a 50% theoretical infill density and different infill patterns. A legend for all bar graphs is shown in (d).

The resulting compressive yield stresses and Young's moduli of scaffold samples under either longitudinal or transverse compression are reported as mean ± standard deviation in **Figure 3**. As shown in **Figure 3 (a)**, the longitudinal yield stresses for PCL and OBC scaffolds with various geometric infills fall in the range of 5-10 MPa. In contrast, the PLA and PLA/PHA scaffolds with different infill geometries exhibit longitudinal yield stresses above 15 MPa, which are significantly higher than those of PCL and OBC scaffolds. Meanwhile, for the same material with same infill geometry, the longitudinal yield stress is overall higher that its transverse yield stress, as shown in **Figure 3(b)**. PLA and PLA/PHA scaffolds also exhibit the higher compressive Young's moduli than PCL and OBC scaffolds, regardless of their infill geometries, as shown in **Figure 3(c)**. For the same material with identical infill geometry, the longitudinal Young's modulus is always higher than its transverse Young's modulus, displaying a trend like

that observed for yield stress. It is worth noting that among all scaffolds printed from the same material, scaffolds with a gyroid infill pattern exhibit minimum differences between longitudinal and transverse yield stresses (and Young's moduli), as highlighted in **Figure 3**. Presumably, this is due to the bicontinuous nature of gyroid infill, which gives rise to isotropic properties for the cubic scaffolds.

In this training module, students first learned to operate the MTS Insight 5 Mechanical testing system and became familiar with the ASTM D 1621 testing standard. Numerous compression tests were performed by trainees to generate data presented in **Figure 3** and to prepare for the Weibull Analysis discussed in Training Module 4. Students mastered the skills necessary to determine the yield stress and the compressive Young's modulus for each scaffold. By having students export raw data into Excel spreadsheets and work with these spreadsheets, students' mathematical computation skills can be enhanced. The ability to plot stress-strain curves using raw data, to calculate mean and standard deviation for stresses and moduli, to generate bar graphs, to compare sets of data (*e.g.*, longitudinal compression vs transverse compression, different infill geometries, different polymers, etc.), and to identify trends and patterns using these graphs and tables are skills that were highlighted.

Training Module 4. Weibull Analysis

Weibull analysis is a statistical method for evaluating life data, analyzing product reliability, and predicting failure trends using constrained data sets.[15–17] The Weibull analysis is performed utilizing the Weibull distribution,[15] viz.,

$$P(\sigma) = 1 - exp\,[-(\sigma/\sigma_o)^m] \qquad \textbf{[Equation (1)]}.$$

In the Weibull distribution function, $P(\sigma)$ is the probability of failure, *i.e.*, the fraction of samples that fail upon compression at or below a given value of applied stress (σ).[15] The term, σ_o, is the characteristic value of the applied stress (*i.e.*, characteristic life) at which 63.2% of the population of the tested samples have failed. Parameter *m* is the Weibull modulus (*i.e.*, shape parameter, not to be confused with physical modulus). Higher Weibull modulus *m* indicates a higher homogeneity of the distribution that correlates to more predictable failure behavior of the tested samples.[15] The Weibull modulus is determined from linear regression ($y = mx + b$), viz.,

$$ln\{ln[1/(1-P(\sigma))]\} = mln(\sigma) - mln(\sigma_o) \qquad \textbf{[Equation (2)]}.$$

In Equation (2), $y = ln\{ln[1/(1-P(\sigma))]\}$, $x = ln(\sigma)$, and $b = -mln(\sigma_o)$. $P(\sigma)$ can be estimated using the Hazen failure probability estimator $P(\sigma) = (i-0.5)/n$, where i is the rank of the data point when all test results are ranked in ascending order and n is the sample size. The Weibull modulus for mechanical testing results obtained in Training Module 3 were calculated by following the Weibull Analysis Procedure (see supporting materials). An example Weibull plot (y vs x) for 30 PCL scaffolds with 50% triangle infill is shown in **Figure 4**. This training module exposed students to intensive mathematical calculation and Excel graphing techniques. All students were trained to perform the Weibull analysis independently and present the results using tables and graphs of professional quality.

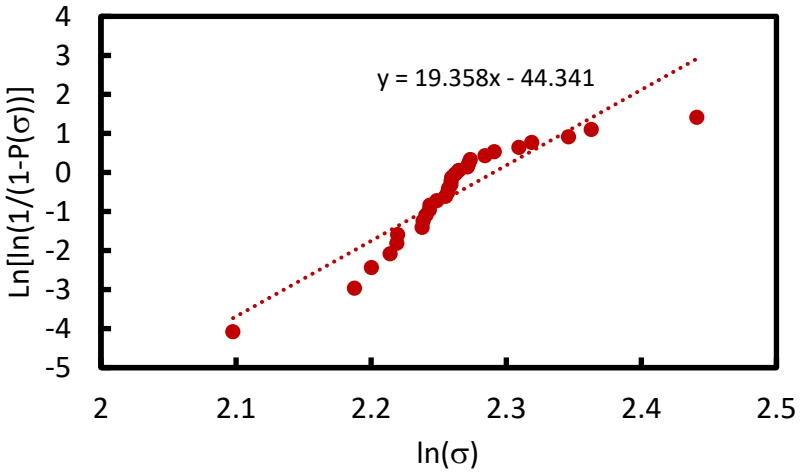

Figure 4. An example of a Weibull plot generated from the longitudinal yield stresses from 30 replicates for a PCL sample with 50% triangle infill.

Table 3. Weibull analysis results for scaffolds with 50% triangle infill.

Material	E_0 (MPa)		σ_0 (MPa)		m
	Longitudinal	Transverse	Longitudinal	Transverse	Longitudinal
PCL	649	396	9.9	4.4	19
OBC	458	417	11.4	7.8	13
PLA	3310	3112	33.4	19.8	12
PLA/PHA	3659	3203	36.3	28.9	16
PVA	157	106	N/A	N/A	N/A

E_0 = characteristic compressive Young's modulus

σ_0 = characteristic yield stress

m = Weibull moduli determined using yield stress data for samples compressed longitudinally.

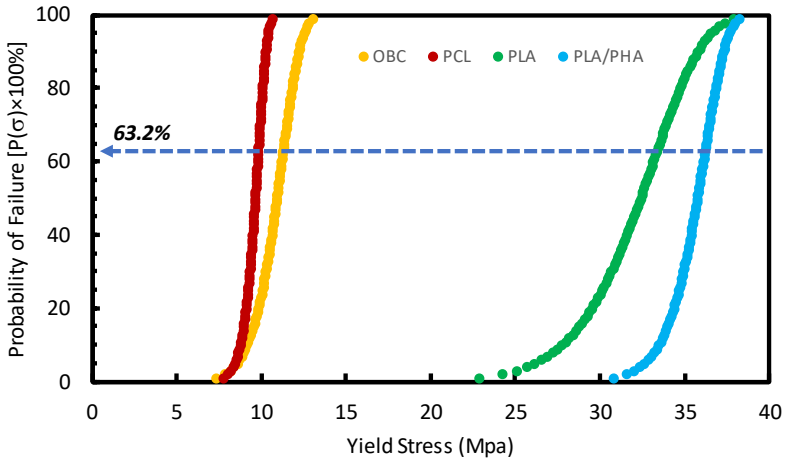

Figure 5. Failure probability vs longitudinal yield stress plots for OBC, PCL, PLA, and PLA/PHA scaffolds with 50% triangle infill.

The Weibull analysis procedure was also adopted to estimate characteristic compressive Young's moduli (E_0) using Young's modulus data. Characteristic compressive Young's moduli (E_0), characteristic yield stresses (σ_0), and Weibull moduli (m) of longitudinal yield stress for all materials with 50% triangle infill are summarized in **Table 3**. [Note: characteristic yield stresses (σ_0) and Weibull moduli (m) of yield stress were not calculated for the PVA samples because no distinct yield stress point was observed.] Under current experimental conditions, PLA/PHA scaffolds with 50% triangle infill exhibit the highest characteristic strength at $P(\sigma)$ = 63.2%, regardless of the compression methods. PCL material exhibits the highest Weibull modulus (m) among all materials tested in this study, indicating more predictable failure behavior of the 3D-printed PCL scaffolds. Probability of failure, $P(\sigma)$, versus yield stress or compressive Young's modulus were also graphed for all materials. As an example, $P(\sigma)$ vs longitudinal yield stress (σ) graphs for OBC, PCL, PLA, and PLA/PHA scaffolds with 50% triangle infill are shown in **Figure 5**. As shown in **Figure 5**, 63.2% of the longitudinally compressed PLA/PHA scaffolds with 50% triangle infill fail at 36.3 MPa, the highest among all materials tested in this study (also see **Table 3**). In contrast, 63.2% of the longitudinally compressed PCL scaffolds failed at 9.9 MPa. Meanwhile, it is also shown in **Figure 5** that the narrowest distribution of the yield stress data for PCL scaffolds, corresponding to the highest Weibull modulus (m = 19) and the most predictable failure behavior of PCL scaffolds among all different scaffolds with 50% triangle infill.

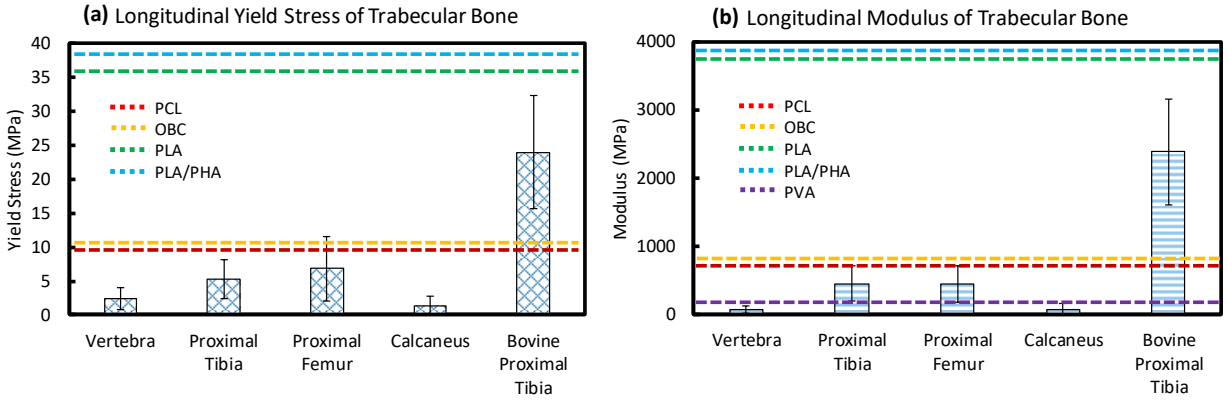

Figure 6. (a) Longitudinal yield stresses and (b) moduli of trabecular bones[18] (bar graphs) and polymer scaffolds with 50% triangle infill prepared in this study (dashed lines).

To compare the mechanical properties of polymer scaffolds prepared in this study with the mechanical properties of bone tissues in different anatomic locations, reported yield stresses and moduli of trabecular bones are plotted in **Figure 6**.[18] The yield stresses and moduli of PCL and OBC scaffolds (see red and orange dashed lines) exhibit the strength that is most comparable to trabecular bones in different anatomic locations, except with that for Bovine proximal tibia. According to the Weibull analysis results, PCL scaffolds also exhibit the most predictable failure behavior among all scaffolds with 50% triangle infill. Predicable failure behavior is crucial for fabricating mechanically reliable biomaterials. Therefore, future training programs will be focused primarily upon 3D printed PCL-based materials, including but not limited to customized composite filaments which incorporate bioactive additives (*e.g.*, hydroxyapatite nanoparticles) into a PCL matrix.

Conclusion

High school seniors gained a good grasp of polymer mechanical properties through the above training modules. Concepts included: (1) PLA and PLA/PHA 3D-printed scaffolds are stiffer than PCL and OBC scaffolds with same infill geometry and density; (2) infill geometry does affect the strength of 3D-printed scaffolds; (3) the scaffold's chemical composition plays a more dominant role in its mechanical properties; (4) the PVA scaffold is the most compliant material

among all samples and no distinct yield stress was observed, regardless of infill geometry; (5), both the longitudinal yield stress and Young's modulus are higher overall than the transverse yield stress and Young's modulus for the same polymeric material; and (6) minimum differences between longitudinal and transverse compressions are observed for scaffolds with gyroid infill. The last observation indicates that bicontinuous gyroid infill geometries could be chosen to print scaffolds with isotropic mechanical properties.

Outcomes

Overall, the summer training program exposed students to interdisciplinary material science and engineering research, with an emphasis on 3D printed polymer scaffolds for bone tissue engineering. Students gained hands-on experience with: (1) operating a differential scanning calorimeter and an MTS Insight 5 electromechanical testing system, (2) conducting CAD design for 3D printing, (3) tabulating, graphing, and reporting research data, (4) learning an application of statistics via performing Weibull analysis, and (5) designing experiments based on trial and error. Students also learned how to perform experiments with statistically sufficient duplication, interpret research results meticulously and critically, and present research results professionally.

The Michigan State University St. Andrews campus that hosted this summer research internship is supported by the Herbert H. and Grace A. Dow Foundation, the Rollin M. Gerstacker Foundation, the Charles J. Strosacker Foundation, and the Dow Chemical Company Foundation. The center offers various STEAM educational programs for K-12 teachers and students throughout the year. More importantly, the center is well-equipped with materials science and engineering research equipment. Several faculty members are experienced PhD-level scientists and engineers. The continuing program, designed based on the research results achieved by 2019 summer interns, will be offered in summer 2020. In addition to a poster presentation, which was required for 2019 summer interns, it is also feasible to require future interns to submit a final report. The research termination papers can be used to measure student learning outcome, such as knowledge, critical reasoning skills, scientific communication and writing skills, and skills to disseminate research findings.

Acknowledgement

The authors thank Dow Chemical Company for the donation of OBC material, Herbert H. and Grace A. Dow Foundation, Rollin M. Gerstacker Foundation, Charles J. Strosacker Foundation and Dow Chemical Company Foundation for their generous financial support.

References

(1) Cameron, J. A.; Milner, D. J.; Lee, J. S.; Cheng, J.; Fang, N. X.; Jasiuk, I. W. Employing the Biology of Successful Fracture Repair to Heal Critical Size Bone Defects. In *Curr Top in Microbiology and Immunol*; Springer: Berlin, Heidelberg, **2013**, **367**, 113–132.

(2) Song, F.; Li, B.; Stocum, D. L. Amphibians as Research Models for Regenerative Medicine. *Organogenesis* **2010**, *6* (3), 141–150.

(3) Nauth, A.; Schemitsch, E.; Norris, B.; Nollin, Z.; Watson, J. T. Critical-Size Bone Defects: Is There a Consensus for Diagnosis and Treatment? *J. Orthop. Trauma* **2018**, *32* (Supplement 3), S7–S11..

(4) Keating, J. F.; Simpson, A. H. R. W.; Robinson, C. M. The Management of Fractures with Bone Loss. *J. Bone Joint Surg. Br.* **2005**, *87-B* (2), 142–150.

(5) Sanders, D. W.; Bhandari, M.; Guyatt, G.; Heels-Ansdell, D.; Schemitsch, E. H.; Swiontkowski, M.; Iii, P. T.; Walter, S. Critical-Sized Defect in the Tibia: Is It Critical? Results From the SPRINT Trial. *J Orthop Trauma* **2014**, *28* (11), 4.

(6) Amini, A. R.; Laurencin, C. T.; Nukavarapu, S. P. Bone Tissue Engineering: Recent Advances and Challenges. *Crit Rev Biomed Eng.* **2012**, *40*(5), 363–408.

(7) Yan, Y.; Chen, H.; Zhang, H.; Guo, C.; Yang, K.; Chen, K.; Cheng, R.; Qian, N.; Sandler, N.; Zhang, Y. S.; et al. Vascularized 3D Printed Scaffolds for Promoting Bone Regeneration. *Biomaterials* **2019**, *190–191*, 97–110.

(8) Udayabhanu Jammalamadaka; Karthik Tappa. Recent Advances in Biomaterials for 3D Printing and Tissue Engineering. *J. Funct. Biomater.* **2018**, *9* (1), 22.

(9) Zhang, L.; Yang, G.; Johnson, B. N.; Jia, X. Three-Dimensional (3D) Printed Scaffold and Material Selection for Bone Repair. *Acta Biomater.* **2019**, *84*, 16–33.

(10) Derby, B. Printing and Prototyping of Tissues and Scaffolds. *Science* **2012**, *338* (6109), 921–926.

(11) Bengtsson, S.; Karlsson, A.; Alexandersson, T.; Quadri, L.; Hjort, M.; Johansson, P.; Morgan-Sagastume, F.; Anterrieu, S.; Arcos-Hernandez, M.; Karabegovic, L.; et al. A Process for Polyhydroxyalkanoate (PHA) Production from Municipal Wastewater Treatment with Biological Carbon and Nitrogen Removal Demonstrated at Pilot-Scale. *New Biotechnol.* **2017**, *35*, 42–53.

(12) ColorFabb Natural PLA/PHA Filament https://www.matterhackers.com/store/l/colorfabb-natural-pla-pha-filament-1.75mm/sk/MKNKADY4.

(13) Dow OBC Filament https://www.matterhackers.com/store/l/dow-obc-filament/sk/MTX3M0TK.

(14) ASTM International, 100 Barr Harbor Drive, PO Box C700, West Conshohocken, PA, 19428-2959 USA.

(15) Kirtay, S.; Dispinar, D. Effect of Ranking Selection on the Weibull Modulus Estimation. *Gazi University Journal of Science*. **2012**, 13. 25(1):175-187.

(16) Askeland, D. R.; Fulay, P. P.; Wright, W. J. *The Science and Engineering of Materials*, 6th ed.; Cengage Learning: Stanford, CT, USA, 2011.
(17) Quinn, J. B.; Quinn, G. D. A Practical and Systematic Review of Weibull Statistics for Reporting Strengths of Dental Materials. *Dent. Mater.* **2010**, *26* (2), 135–147.
(18) Keaveny, T. M.; Morgan, E. F.; Niebur, G. L.; Yeh, O. C. Biomechanics of Trabecular Bone. *Annu. Rev. Biomed. Eng.* **2001**, *3* (1), 307–333.

Supporting Materials

I. Weibull Analysis Procedure

The Weibull modulus is determined from linear regression ($y = mx + b$), viz.,

$$ln\{ln[1/(1 - P(\sigma))]\} = mln(\sigma) - mln(\sigma_o).$$[15]

In above equation, $y = ln\{ln[1/(1 - P(\sigma))]\}$, $x = ln(\sigma)$, and $b = -mln(\sigma_o)$. $P(\sigma)$ can be estimated using the Hazen failure probability estimator $P(\sigma) = (i - 0.5)/n$, where *i* is the rank of the data point when all test results are ranked in ascending order and *n* is the sample size. To calculate the Weibull modulus for mechanical testing results obtained in Training Module 3, yield stresses (σ) determined from stress-strain curves for 30 scaffold samples were recorded in the ***1st column*** and sorted in ascending order with the ranking order (*i*) recorded in the ***2nd column***. Students then calculated the estimated failure probability using $P(\sigma) = (i - 0.5)/n$ with a sample size $n = 30$. The results ($P(\sigma)$ were then recorded in the ***3rd column***. The values of *y* and *x* were calculated using equations: $y = ln\{ln[1/(1 - P(\sigma))]\}$ and $x = ln(\sigma)$, respectively, and recorded in the ***4th and 5th columns***, respectively. For each set of 30 samples, one scatter plot can be generated with $y = ln\{ln[1/(1 - P(\sigma))]\}$ and $x = \ln(\sigma)$. Linear regression was then performed to determine the Weibull modulus (*m*), *i.e.*, the slope of the linear trend line, and the characteristic yield stress, $\sigma_o = exp(-b/m)$, where *b* is the *y*-intercept of the linear trend line.

II. Stress-strain curves of OBC and PVA scaffolds with 50% triangle infill.

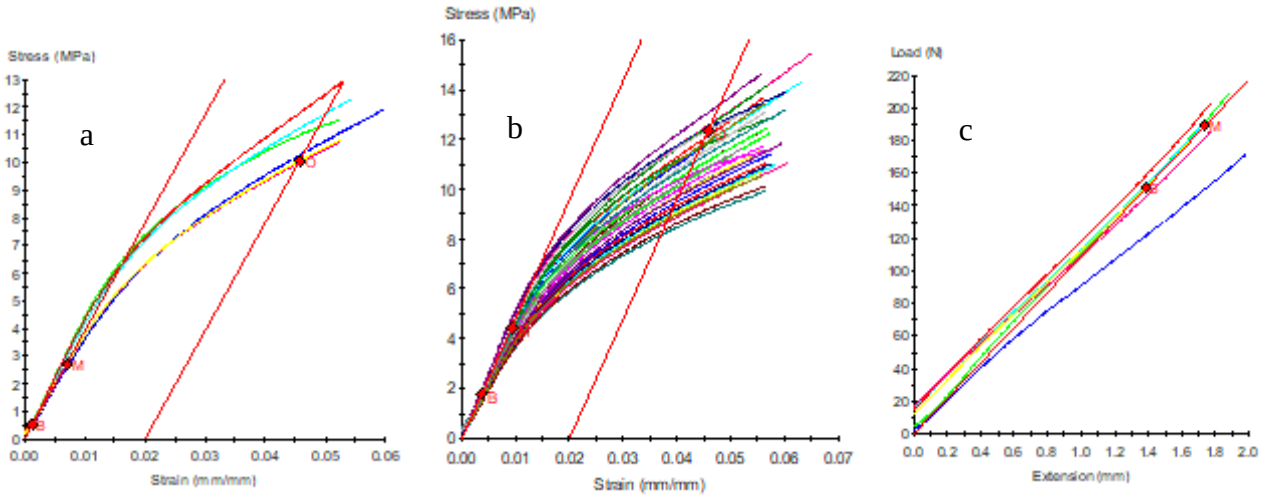

Figure S1. Stress-strain curves of (a and b) OBC and (c) PVA scaffolds with 50% triangle infill: (a) overlaid 6 curves to determine the compressive modulus and yield stress of OBC scaffold, (b) overlaid 30 curves for performing Weibull analysis for OBC scaffolds, and (c) overlaid 6 curves to determine the compressive modulus and yield stress of PVA scaffolds.